On-Demand Production of Flow-Reactor Cartridges by 3D Printing of Thermostable Enzymes

*Manfred Maier, Carsten P. Radtke, Jürgen Hubbuch, Christof M. Niemeyer, and Kersten S. Rabe**

Abstract: *The compartmentalization of chemical reactions is an essential principle of life that provides a major source of innovation for the development of novel approaches in biocatalysis. To implement spatially controlled biotransformations, rapid manufacturing methods are needed for the production of biocatalysts that can be applied in flow systems. Whereas three-dimensional (3D) printing techniques offer high-throughput manufacturing capability, they are usually not compatible with the delicate nature of enzymes, which call for physiological processing parameters. We herein demonstrate the utility of thermostable enzymes in the generation of biocatalytic agarose-based inks for a simple temperature-controlled 3D printing process. As examples we utilized an esterase and an alcohol dehydrogenase from thermophilic organisms as well as a decarboxylase that was thermostabilized by directed protein evolution. We used the resulting 3D-printed parts for a continuous, two-step sequential biotransformation in a fluidic setup.*

The compartmentalization of (bio)chemical reactions is a fundamental principle of life, bearing great potential for synthetic chemistry. Hence, this field is an area of intense research and development, and has attracted much attention in the past years.[1–7] Performing multistep biotransformations with a defined sequence of biocatalysts can circumvent challenges such as incompatible reaction conditions, unwanted side reactions, and product inhibition. However, all established state-of-the-art technologies used to arrange enzymes for sequential reactions require significant chemical or genetically encoded modifications of the target enzymes.[8–11] As a result, the activities and specificities of the enzymes can be negatively influenced.

To create defined spatial arrangements, the biocatalyst can also be directly immobilized by encapsulation in a carrier material, which can also stabilize the biocatalyst.[12,13] Indeed, several strategies have been used for the mild encapsulation of enzymes and cells in natural and synthetic polymers.[14–18] However, these materials do not usually meet the requirements of advanced manufacturing processes such as three-dimensional (3D) printing. Methods for the printing of enzyme-containing polymer mixtures have been described,[19–21] but require sophisticated lithography instrumentation, additional components such as photoinitiators, or post-printing treatments and/or sacrificial scaffold materials. Extrusion-based printers are simpler and more widespread in state-of-the-art academic and industrial settings.[22–24] However, this 3D printing strategy requires the development of bioinks with suitable physiochemical parameters for both the enclosed enzymes and the printing process.[25] In the case of simple syringe-based extrusion printing without post-print processing steps, elevated temperatures are necessary, and these are not compatible with all enzymes. Therefore, to the best of our knowledge, a direct ink writing process using an enzyme-containing bioink in a standard, syringe-based extrusion printer has yet to be realized.

We herein demonstrate that thermostable enzymes can be harnessed to realize an easy-to-handle 3D printing process. A simple and inexpensive, agarose-based, thermoreversible, enzyme-integrated hydrogel was used for the convenient production of flow-reactor cartridges. The resulting biocatalytic modules were composed of only the enzyme and an inexpensive biomaterial (agarose), they can be produced on-demand, on-site, and are biodegradable after use. In this approach, solely the thermostability of the target enzyme is important as the enzyme needs to withstand the elevated temperatures required for the processing of the biocatalytic ink, which is the sole treatment of the ink during the whole 3D printing process. For this purpose, either native enzymes from the rich source of naturally occurring thermostable organisms can be used (the BRENDA database alone contains 1275 enzymes with an experimental thermostability of $> 60\,°C$),[26] or conventional enzymes from mesophilic organisms can be rendered thermostable for specific applications by means of established protein engineering methods.[27–36] In a proof-of-concept study, we demonstrate the versatility of this approach by using esterase or alcohol dehydrogenase wild-type enzymes from thermophilic organisms as well as a decarboxylase from a mesophilic source that has been engineered for increased thermostability. The application of these bioinks in a 3D printing process enabled the straightforward fabrication of flow-reactor cartridges, which were used for modular, tunable, two-step biotransformations under continuous-flow conditions even in THF/buffer mixtures, which are otherwise detrimental to the enzyme activity.

[*] M. Sc. M. Maier, Prof. Dr. C. M. Niemeyer, Dr. K. S. Rabe
Karlsruhe Institute of Technology (KIT)
Institute for Biological Interfaces (IBG 1)
Herrmann-von-Helmholtz-Platz 1
76344 Eggenstein-Leopoldshafen (Germany)
E-mail: kersten.rabe@kit.edu
Dipl.-Ing. C. P. Radtke, Prof. Dr. J. Hubbuch
Karlsruhe Institute of Technology (KIT)
Institute for Engineering in Life Science
Section IV: Biomolecular Separation Engineering
Fritz-Haber-Weg 2, 76131 Karlsruhe (Germany)

We initially established experimental procedures for temperature controlled 3D printing utilizing 3 % (w/v) agarose hydrogels that can be prefabricated and stored inside the printer cartridges.[37,38] To ensure broad applicability, we used a commercially available 3D printer (BioScaffolder 3.1, GeSiM) equipped with a pneumatic, heatable print head and a cooled print surface (Peltier cooler), enabling the layer by layer fabrication of defined 3D scaffolds. We printed different grid structured circles and polygons with diameters of 10 20 mm and heights of 5 mm (Figure 1). The scaffolds could be printed in a highly reproducible manner, and the design shown in Figure 1B,C was chosen to match the requirements for a flow reactor in terms of size, geometry, and optimized flow rates and back pressure.

Aside from high throughput manufacturing, this 3D printing approach also allows for the rapid prototyping of devices to enable systematic screens for optimal buffer conditions, scaffold materials, and their concentrations to meet the distinctive requirements of the enzymes of interest and/or to optimize the shape and surface/volume aspects of the discs for optimal reactor performance. To study the suitability of thermostable enzymes as functional biocatalytic components of the agarose ink, we prepared individual agarose hydrogels containing an esterase (EstII) or an alcohol

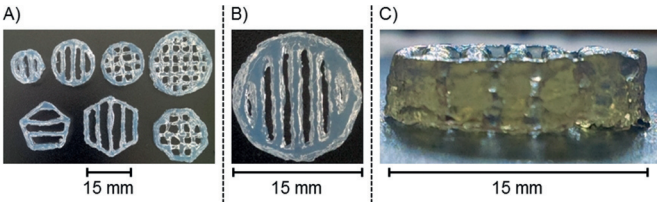

Figure 1. 3D printed grid structured scaffolds based on 3 % (w/v) agarose hydrogels. A) Different shapes and sizes can be printed. B) Top view and C) side view of the scaffold used in the flow reactor setup.

dehydrogenase (ADH)[39,40] from the thermophilic organism *Alicyclobacillus acidocaldarius*. Both enzymes show high T_{50} values, a quantitative measure for thermostability,[41] indicating the distinct thermostability of the chosen biocatalysts (Figure 2A). The agarose hydrogels were prepared in advance from liquid agarose (42 °C) and the purified enzyme (2 μM end concentration) to give the bioinks, which could be stored for prolonged periods of time (Supporting Information, Figure S1) inside the print cartridge and used on demand for the 3D printing of the desired scaffolds.

We initially analyzed whether the thermophilic EstII and ADH enzymes indeed withstand the printing procedure and

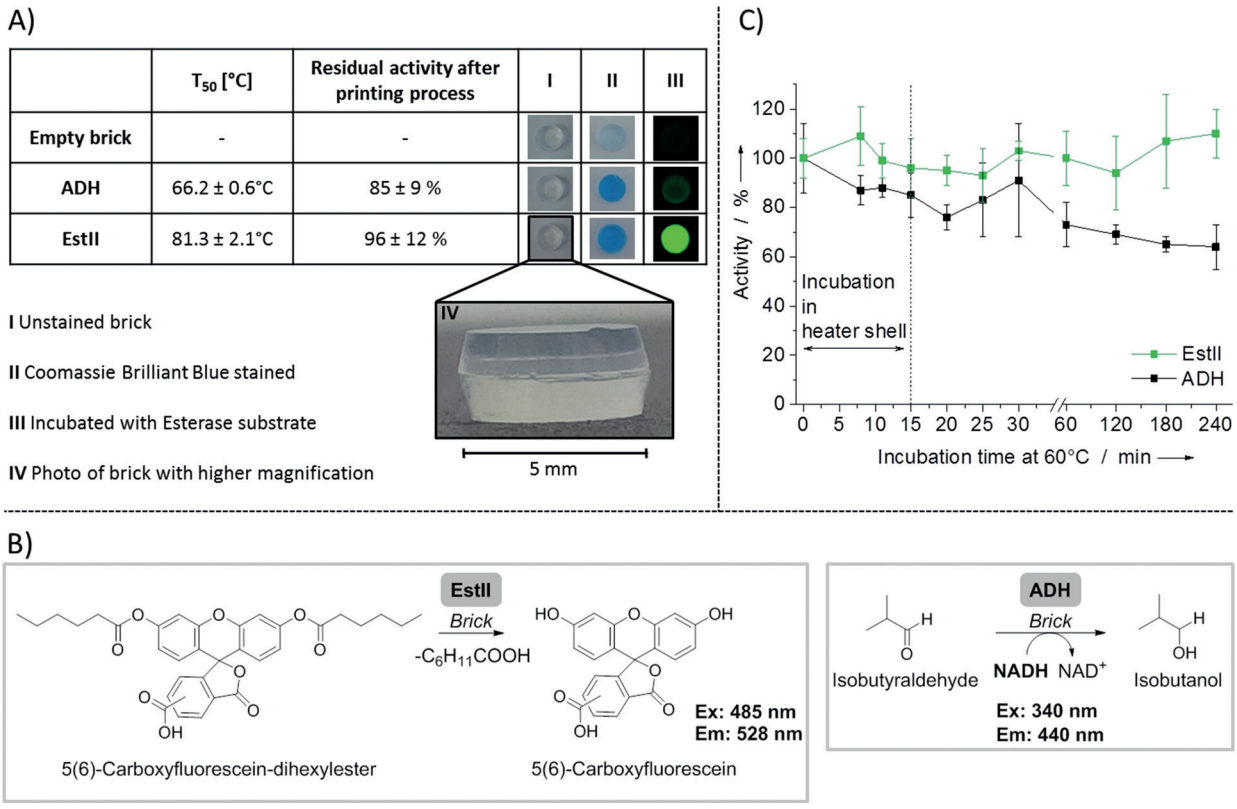

Figure 2. A) Comparison of the thermophilic enzymes ADH and EstII in terms of the T_{50} values and residual activities [%] of the corresponding bioinks after incubation at 60 °C for 15 min (incubation temperature and time in the 3D printing process), normalized to the activity determined for freshly prepared bioinks. The activities were determined by using hardened agarose samples (bricks), as shown in I and IV. Column II visualizes the enzyme load of the bricks by Coomassie Brilliant Blue staining. Column III shows bricks that were incubated with the fluorogenic EstII substrate (shown in B). B) Fluorogenic reactions used for determining the activity of ADH and EstII. C) Activity of enzyme loaded bricks as a function of the incubation time of the gel samples at 60 °C, representing the incubation temperature for re melting of the bioink in the 3D printing process. Data are normalized to the respective activities of freshly prepared bioinks. The error bars in (C) represent the standard deviations of at least two experimental replicates.

stay functional throughout the melting process in the heater shell of the 3D printer by incubating samples of the bioinks at 60 °C in a thermoblock and subsequent molding into cylindrical bricks (5 mm × 2.7 mm; Figure 2A and Figure S2). The enzyme loads of these bricks (57.2 ± 0.7 mg agarose hydrogel, 2 μM enzyme) were clearly visualized by staining with Coomassie Brilliant Blue or incubation of the EstII loaded brick in a solution containing the fluorogenic substrate 5(6) carboxyfluorescein dihexylester (Figure 2A). For a more detailed characterization, the enzyme loaded bricks were analyzed in terms of the EstII catalyzed de esterification of the fluorescein derivative and an ADH catalyzed reduction to yield isobutanol (Figure 2B). As shown in Figure 2C, the thermostable enzymes could be incubated at 60 °C for 240 min without a significant loss of activity. These results provided initial support for our hypothesis that thermostable enzymes could be used for 3D printing applications as the 15 min incubation at 60 °C needed for the printing process did not substantially harm the enzymes.

As specific applications might require the employment of enzymes of which thermostable variants have not yet been described, we next demonstrated that the physical properties of a mesophilic enzyme can be adjusted by established protein engineering methods to render it suitable for the 3D printing process described above. As a model enzyme, we used the ketoisovalerate decarboxylase[42,43] (KIVD) from the mesophilic organism *Lactococcus lactis* because the thermostabilization of this cofactor dependent, homodimeric enzyme with two active sites at the monomer monomer interface is challenging. The thermostabilized variant, in the following referred to as KIVD mutant, contains three amino acid substitutions as compared to the wild type sequence (E156K, N351D, S385M). The KIVD mutant ($T_{50} = 61.9 \pm 0.2$ °C) was obtained by directed evolution of the wild type enzyme ($T_{50} = 53.1 \pm 1.5$ °C) by a first round of optimization by computational methods and a second round employing random mutagenesis and screening of a clone library (Figure 3A; see the Supporting Information and Figure S3 for details).

During the detailed characterization of the stabilized KIVD variants, we also analyzed the decarboxylation reaction of ketoisovalerate at 60 °C, which confirmed the enhanced stability and activity at elevated temperatures (Figure S4). The detailed procedure is described in the Supporting Information.

For initial experiments, the KIVD mutant and the wild type enzyme were encapsulated in agarose bricks, and the residual activities after printing were analyzed. To this end, the decarboxylation of ketoisovalerate to isobutyraldehyde was quantified by HPLC analysis (Figure S5). Whereas we were not able to detect any decarboxylation products of ketoisovalerate in the case of the wild type KIVD bricks, the KIVD mutant bricks showed substantial activity (36 ± 7 %) after the printing procedure (Figure 3A). This result clearly confirmed that, if required, mesophilic enzymes can indeed be readily optimized by directed evolution to become applicable for such 3D printing processes that are based on temperature dependent gelation of the bioink.

With the engineered KIVD mutant in hand, we produced 3D printed grid structured discs (Figure 1B,C), with dimensions fitting in a simple flow reactor. The flow reactor comprises a cartridge that can hold various numbers of agarose discs and is connected via tubing to a syringe pump that delivers the substrate solution (Figure 3B). An initial system containing one KIVD mutant disc was operated in upflow mode at a flow rate of 25 μL min^{-1}, and the outflow was analyzed by HPLC (Figure 3C). The formation of isobutyraldehyde from ketoisovalerate (10 mM provided in the inflow) reached a constant level after about 40 min, with a maximum concentration of 4.1 ± 0.2 mM isobutyraldehyde in the outflow.

We also investigated to which extent enzymes are washed out of the agarose matrix during flow operation. Western blot analysis of the outflow revealed molecular weight dependent elution behavior (Figure 3D and Figure S6). Based on these data, operational volumes of up to 70 mL of product were estimated for the present setting, which could be further optimized by changes in the agarose concentration, the specific design of the surface and volume of the printed discs, as well as the operational flow rates. We also established that the incorporation into the agarose matrix leads to significant protection of the enzymes against organic solvents. Whereas the EstII enzyme dissolved in solution was already inactive in solvents containing more than 20 % (v/v) THF in the buffer, the enzyme embedded in the agarose gel still showed significant catalytic activity at up to 40 % (v/v) THF/buffer (Figure S7).

To confirm that several agarose discs can be conveniently combined in a modular fashion, a fluidic system (Figure 3B) was assembled that catalyzes the two step biotransformation of ketoisovalerate into isobutanol (Figure 3E). The reactor was perfused in upflow mode at a flow rate of 25 μL min^{-1}, and the formation of isobutanol was quantified by HPLC analysis (Figure S8). As shown in Figure 3E, the increase in the concentration of isobutanol in the outflow correlated with the increase in the number of ADH discs, leading to the formation of isobutanol in concentrations of up to 0.4 mM (1 ADH disc), 0.6 mM (2 discs), or 0.8 mM (3 discs). These results clearly demonstrate the modularity of the system, which enables a simple approach for the sequential coupling of biotransformations with concomitant tuning of the product concentration in the outflow. The exemplary 3D printed agarose hydrogel structures shown here enable the direct flow of the substrate solution inside the reactor and rapid diffusion into the gel with an estimated rate of 100 μm s^{-1} (Figure S9). Owing to the implementation of the effective 3D printing technique presented here, the geometry of the scaffolds can be easily modified. When several discs are used, they can also be arranged with a small, grid related offset to prevent direct flow through the gaps of the present design.

In conclusion, we have demonstrated that thermostable enzymes can be advantageously used for novel bioinks that enable the facile fabrication of modular biocatalytic flow systems by means of 3D printing processes. In contrast to other systems, our approach depends solely on the thermostability of the target enzymes, and it is thus particularly suited for the rapid prototyping and manufacturing of biocatalytic flow systems. In this way, cascaded reaction setups for multistep biotransformations using a single flow

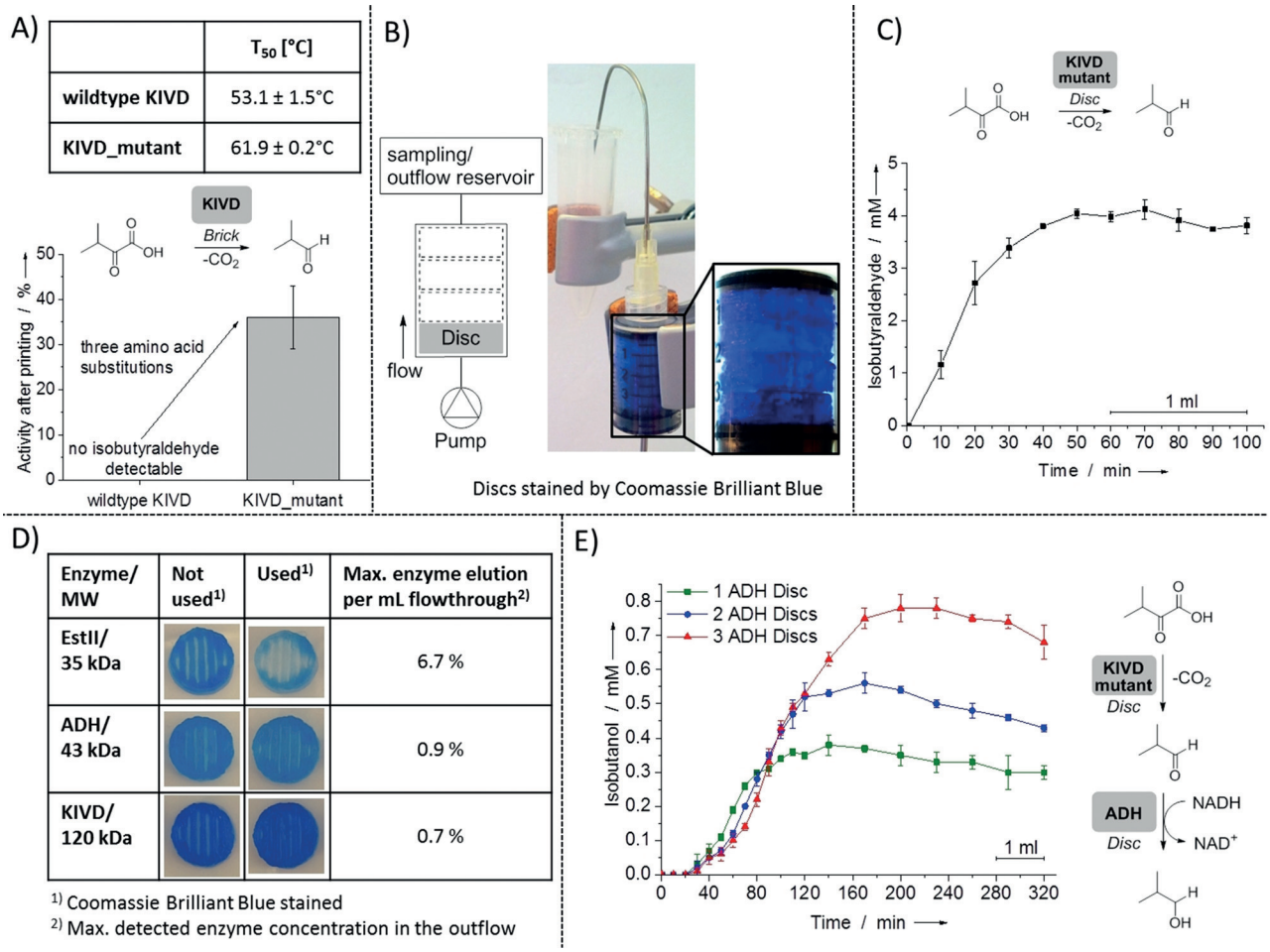

Figure 3. A) Comparison of wild type KIVD and the KIVD mutant in terms of the T_{50} values and the residual activities [%] of the bioinks before and after the printing process. B) Schematic representation and photographic image of a fluidic system used for this study. For better visualization, enzyme loaded discs were stained with Coomassie Brilliant Blue. C) Concentration of isobutyraldehyde in the outflow of the flow reactor containing one KIVD mutant disc as a function of time. D) Coomassie Brilliant Blue stained discs that either were fresh or had been used in fluidic experiments revealed molecular weight dependent enzyme elution from the agarose matrix. E) Time dependence of the concentration of isobutanol in the outflow of the fluidic system comprising one KIVD mutant disc in combination with one (green), two (blue), or three (red) ADH discs. NADH was constantly provided in the reaction buffer. Note that the concentration of isobutanol in the outflow correlates with the number of ADH discs employed. The error bars in (A), (C), and (E) represent the standard deviation of at least two experimental replicates.

chamber can be realized and optimized without the need for multiple orthogonal immobilization strategies. The number of available thermostable enzymes is steadily increasing,[44] and regular enzymes from mesophilic sources can also be adapted to higher process temperatures, as indicated by the develop ment of the KIVD mutant. The method described here is not restricted to certain buffer conditions and allows for the fabrication of arbitrarily shaped 3D structures. Furthermore, agarose, the sole material that is needed for the reported 3D printing technique, is a very inexpensive and non toxic material, facilitating the preparation, storage, transportation, and disposal of the enzyme containing bioink. We therefore believe that our technology has the potential to pave new ways for the implementation of added manufacturing tech niques in biocatalysis and, in the long run, to enable the establishment of automated, machine assisted bioproduction processes.[45]

Acknowledgements

We acknowledge financial support of this work by the Helmholtz program “BioInterfaces in Technology and Med icine”. We thank Yong Hu and Lukas Wenger for their experimental help.

Conflict of interest

The authors declare no conflict of interest.

Keywords: 3D printing · directed evolution · enzymes · flow chemistry · gels

[1] I. Wheeldon, S. D. Minteer, S. Banta, S. C. Barton, P. Atanassov, M. Sigman, *Nat. Chem.* **2016**, *8*, 299.
[2] A. Küchler, M. Yoshimoto, S. Luginbuhl, F. Mavelli, P. Walde, *Nat. Nanotechnol.* **2016**, *11*, 409.
[3] J. H. Schrittwieser, S. Velikogne, M. Hall, W. Kroutil, *Chem. Rev.* **2018**, *118*, 270.
[4] C. Hold, S. Billerbeck, S. Panke, *Nat. Commun.* **2016**, *7*, 12971.
[5] D. N. Tran, K. J. Balkus, *ACS Catal.* **2011**, *1*, 956.
[6] R. A. Sheldon, S. van Pelt, *Chem. Soc. Rev.* **2013**, *42*, 6223.
[7] P. Gruber, M. P. C. Marques, B. O'Sullivan, F. Baganz, R. Wohlgemuth, N. Szita, *Biotechnol. J.* **2017**, *12*, 1700030.
[8] S. Costa, A. Almeida, A. Castro, L. Domingues, *Front. Microbiol.* **2014**, *5*, 63.
[9] K. Terpe, *Appl. Microbiol. Biotechnol.* **2003**, *60*, 523.
[10] P. Jonkheijm, D. Weinrich, H. Schröder, C. M. Niemeyer, H. Waldmann, *Angew. Chem. Int. Ed.* **2008**, *47*, 9618; *Angew. Chem.* **2008**, *120*, 9762.
[11] E. Peris, O. Okafor, E. Kulcinskaja, R. Goodridge, S. V. Luis, E. Garcia Verdugo, E. O'Reilly, V. Sans, *Green Chem.* **2017**, *19*, 5345.
[12] S. R. Caliari, J. A. Burdick, *Nat. Methods* **2016**, *13*, 405.
[13] Y. Lv, T. Tan, F. Svec, *Biotechnol. Adv.* **2013**, *31*, 1172.
[14] M. T. Reetz, *Adv. Mater.* **1997**, *9*, 943.
[15] C. Li, A. Faulkner Jones, A. R. Dun, J. Jin, P. Chen, Y. Xing, Z. Yang, Z. Li, W. Shu, D. Liu, R. R. Duncan, *Angew. Chem. Int. Ed.* **2015**, *54*, 3957; *Angew. Chem.* **2015**, *127*, 4029.
[16] L. Gasperini, J. F. Mano, R. L. Reis, *J. R. Soc. Interface* **2014**, *11*, 20140817.
[17] R. Fan, M. Piou, E. Darling, D. Cormier, J. Sun, J. Wan, *J. Biomater. Appl.* **2016**, *31*, 684.
[18] H. W. Kang, S. J. Lee, I. K. Ko, C. Kengla, J. J. Yoo, A. Atala, *Nat. Biotechnol.* **2016**, *34*, 312.
[19] C. D. Blanchette, J. M. Knipe, J. K. Stolaroff, J. R. DeOtte, J. S. Oakdale, A. Maiti, J. M. Lenhardt, S. Sirajuddin, A. C. Rose nzweig, S. E. Baker, *Nat. Commun.* **2016**, *7*, 11900.
[20] C. A. Mandon, L. J. Blum, C. A. Marquette, *Anal. Chem.* **2016**, *88*, 10767.
[21] C. P. Radtke, N. Hillebrandt, J. Hubbuch, *J. Appl. Chem. Biotechnol.* **2017**, *92*.
[22] S. Kyle, Z. M. Jessop, A. Al Sabah, I. S. Whitaker, *Adv. Healthcare Mater.* **2017**, *6*, 1700264.
[23] R. R. Jose, M. J. Rodriguez, T. A. Dixon, F. Omenetto, D. L. Kaplan, *ACS Biomater. Sci. Eng.* **2016**, *2*, 1662.
[24] M. Guvendiren, J. Molde, R. M. D. Soares, J. Kohn, *ACS Biomater. Sci. Eng.* **2016**, *2*, 1679.
[25] J. Malda, J. Visser, F. P. Melchels, T. Jungst, W. E. Hennink, W. J. Dhert, J. Groll, D. W. Hutmacher, *Adv. Mater.* **2013**, *25*, 5011.
[26] I. Schomburg, A. Chang, C. Ebeling, M. Gremse, C. Heldt, G. Huhn, D. Schomburg, *Nucleic Acids Res.* **2004**, *32*, D431 D436.
[27] O. Buss, D. Muller, S. Jager, J. Rudat, K. S. Rabe, *ChemBioChem* **2018**, *19*, 379.
[28] R. Sterner, W. Liebl, *Crit. Rev. Biochem. Mol. Biol.* **2001**, *36*, 39.
[29] H. Yang, L. Liu, J. Li, J. Chen, G. Du, *ChemBioEng Rev.* **2015**, *2*, 87 94.
[30] K. Solanki, W. Abdallah, S. Banta, *Biotechnol. J.* **2016**, *11*, 1483.
[31] H. P. Modarres, M. R. Mofrad, A. Sanati Nezhad, *RSC Adv.* **2016**, *6*, 115252.
[32] B. Steipe, *Methods Enzymol.* **2004**, *388*, 176.
[33] A. S. Bommarius, M. F. Paye, *Chem. Soc. Rev.* **2013**, *42*, 6534.
[34] M. Lehmann, M. Wyss, *Curr. Opin. Biotechnol.* **2001**, *12*, 371.
[35] K. Steiner, H. Schwab, *Comput. Struct. Biotechnol. J.* **2012**, *2*, e201209010.
[36] H. J. Wijma, R. J. Floor, D. B. Janssen, *Curr. Opin. Struct. Biol.* **2013**, *23*, 588.
[37] R. Landers, U. Hubner, R. Schmelzeisen, R. Mulhaupt, *Biomaterials* **2002**, *23*, 4437.
[38] A. C. Daly, S. E. Critchley, E. M. Rencsok, D. J. Kelly, *Biofabrication* **2016**, *8*, 45002.
[39] D. E. Agafonov, K. S. Rabe, M. Grote, Y. W. Huang, M. Sprinzl, *FEBS Lett.* **2005**, *579*, 2082.
[40] P. P. Lin, K. S. Rabe, J. L. Takasumi, M. Kadisch, F. H. Arnold, J. C. Liao, *Metab. Eng.* **2014**, *24*, 1.
[41] S. Lutz, U. T. Bornscheuer, *Protein engineering handbook*, *Vol. 3*, Wiley VCH, Weinheim, **2012**.
[42] C. L. Berthold, D. Gocke, M. D. Wood, F. J. Leeper, M. Pohl, G. Schneider, *Acta Crystallogr. Sect. D* **2007**, *63*, 1217.
[43] M. Beigi, E. Gauchenova, L. Walter, S. Waltzer, F. Bonina, T. Stillger, D. Rother, M. Pohl, M. Muller, *Chem. Eur. J.* **2016**, *22*, 13999.
[44] M. E. DeCastro, E. Rodriguez Belmonte, M. I. Gonzalez Siso, *Front. Microbiol.* **2016**, *7*, 1521.
[45] K. S. Rabe, J. Muller, M. Skoupi, C. M. Niemeyer, *Angew. Chem. Int. Ed.* **2017**, *56*, 13574; *Angew. Chem.* **2017**, *129*, 13760.